Bulletin of Engineering Geology and the Environment (2021) 80:717–729
https://doi.org/10.1007/s10064-020-01959-9

ORIGINAL PAPER

Factors affecting the soil–water retention curve of Chinese loess

Fanyu Zhang [1,2] · Chongxi Zhao [1,2] · Sérgio D. N. Lourenço [3] · Simeng Dong [4] · Yao Jiang [5,6]

Received: 7 April 2020 / Accepted: 7 August 2020 / Published online: 18 August 2020

Abstract

Loess is unsaturated soil that occurs in various locations on the surface of the Earth, and it is most widespread in the Chinese Loess Plateau where it has caused many geotechnical problems and geohazards. To better understand the properties of unsaturated loess, it is helpful to examine its soil–water retention curve (SWRC). In this study, a volumetric pressure plate extractor was used to examine undisturbed, artificial, and remolded loess specimens to investigate the effects of the sampling site, structure disturbance, grain size, and salt solution on their SWRCs. To better analyze the changes in the SWRCs of the loess samples, we also determined their index properties, mineral compositions, specific surface areas (SSAs), cation exchange capacities (CECs), and scanning electron microscopy (SEM). The results showed that the factors that affected their SWRCs mainly were attributable to changes in the microstructure that resulted from differences in their physical natures, physical states, and salt solutions. Also, there has a close link between the macroscopic soil–water retention curves and the microscopic structure characteristics of the loess samples.

Keywords Soil–water retention curve · Loess · Physical nature · Physical state · Structure disturbance · Salt solution

Introduction

Loess is typically unsaturated soil on the Earth's surface, and it occurs extensively on the Chinese Loess Plateau. That location has had many geotechnical problems and geohazards, such as landslides, erosion, and settlement (Derbyshire 2001; Dijkstra et al. 2014; Zhang et al. 2018; Juang et al. 2019). Recently, land-creation projects have been launched by cutting off hilltops and filling valleys in the Chinese Loess Plateau (Zhang and Wang 2018; Zhang et al. 2019). These mega-engineering projects have created large areas of level ground for construction and agricultural activities (Juang et al. 2019). As a result, the natural loess has undergone serious structural disturbances due to cutting, reconstitution, and compaction. One of the vital tasks relative to the unsaturated soil is to describe its behavior and properties by using SWRCs (Fredlund and Rahardjo 1993; Lu and Likos 2004). Hence, understanding the SWRCs of the unsaturated loess undoubtedly is of practical importance for solving geotechnical problems and mitigating geohazards.

The Chinese Loess Plateau is covered by sandy loess, silty loess, and clayey loess (Lin and Liang 1982; Liu 1985; Derbyshire, 2011), each of which has SWRCs that obviously are quite different (Fredlund and Xing 1994; Leong and Rahardjo 1997). Thus, various studies have developed different models to predict the SWRCs of the three types of soils (Brooks and Corey 1966; van Genuchten 1980; Fredlund and Xing 1994; Aubertin et al. 2003). In these studies, the sand had a steep drying curve that had an unsmooth inverse S-shape. However, the silt had a flat and smooth inverse S-shape curve, and the clay had a curve that resembled a

Electronic supplementary material The online version of this article (https://doi.org/10.1007/s10064-020-01959-9) contains supplementary material, which is available to authorized users.

✉ Fanyu Zhang
zhangfy@lzu.edu.cn

[1] MOE Key Laboratory of Mechanics on Disaster and Environment in Western China, Lanzhou University, Lanzhou 730000, Gansu, China

[2] College of Civil Engineering and Mechanics, Lanzhou University, Lanzhou 730000, Gansu, China

[3] Department of Civil Engineering, The University of Hong Kong, Pokfulam Road, Pok Fu Lam, Hong Kong Special Administrative Region, China

[4] Civil Engineering Department, Sichuan College of Architectural Technology, Deyang 618000, Sichuan, China

[5] Key Laboratory of Mountain Hazards and Surface Process, Institute of Mountain Hazards and Environment, Chinese Academy of Sciences, Chengdu 610041, Sichuan, China

[6] CAS Center for Excellence in Tibetan Plateau Earth Sciences, Chinese Academy of Sciences (CAS), Beijing 100101, China

parabola. The changes in types of soil determine its physical nature, physical state, and structure. Generally, the physical natures of soils are related to the constitution of the soil, such as its mineral composition, fine-grain fraction, and the shape of the grains. The physical state of the soil refers to its physical parameters, such as its water content, density, and stress history (Cubrinovski and Ishihara 2002; Yilmaz and Mollamahmutoglu 2009). Essentially, the term "structure" refers to the combination of fabric, composition, and interparticle forces (D'Elia and Picarelli 1998; Feda 2004). Previous studies found that these factors have significant effects on the SWRC of the soil (Fredlund and Rahardjo 1993; Lu and Likos 2004). Some studies also found that the clay mineral compositions, such as montmorillonite, illite, and gypsum, can affect the content of residual water and the air-entry value due to their different hydrophilic properties (Aldaood et al. 2015; Pedarla et al. 2015). Also, the grain size fractions and grain surface characteristics can change the slope, water retention, and air-entry value of the SWRCs (Oades and Waters 1991; James et al. 1997; Zapata et al. 2000; Puppala et al. 2006; Rahardjo et al. 2012; Lourenço et al. 2017). Also, the shapes of the SWRCs have been found to be related to the physical state of the soil, e.g., its initial dry density, water content, and deformation history (Gallipoli et al. 2003; Tarantino 2009; Muñoz-Castelblanco et al. 2012; Ng et al. 2016; Jiang et al. 2017; Mu et al. 2020). Huang et al. (2010) and Zhang et al. (2007) performed tests to determine the SWRCs of the natural loess taken from different soil types in the Chinese Loess Plateau. They used pedotransfer functions to estimate the SWRCs of the loess based on its grain size distribution and its other basic properties. It also was observed via in situ monitoring that the change in the type of soil has a striking influence on the SWRCs of the natural loess samples (Li et al. 2016). In addition, the initial dry density and water content have impacts on the desaturation zones of the SWRCs of the remolded loess (Jiang et al. 2017). Even though much is known, there is still a need to improve our understanding of both natural and remolded loess based on the differences that have been observed in the physical state and structure of the loess.

The properties and behavior of loess change readily due to structural changes, which commonly are related to disturbances or the wetting–drying cycle. It was found in previous studies that changes in the structure of loess produce apparent differences in the SWRCs of natural, remolded, and compacted loess (Muñoz-Castelblanco et al. 2012; Ng et al. 2016; Li et al. 2018; Mu et al. 2020). These studies also showed that slight changes in the structure could result in obvious adjustments of the micropores, causing the different SWRCs of the samples of loess. Some researchers found that the structural changes also have significant influences on the shear strength and consolidation behavior of natural and remolded loess (Zlatovic and Ishihara 2008; Jiang et al. 2012; Liu et al. 2016). It is obvious that the current land-creation projects inevitably have disturbed and remolded the structure of the natural loess in the Chinese Loess Plateau (Zhang et al. 2019). Hence, it still is necessary to perform systematic comparisons of the SWRCs of both the natural and remolded loess because they are characteristic of spatio-temporal features, i.e., typical spatial sites and soil layers.

The loess in the Chinese Loess Plateau contains some salts (Lin and Liang 1982; Liu 1985). Studies have shown that salt solutions have an excellent effect on the mechanical and infiltration behaviors of loess (Dijkstra et al. 1994; Wen and He 2012; Zhang et al. 2013, 2014; Zhang and Zhang 2018). Also, artificial irrigation induced severe soil salinization in the agricultural regions where loess was prevalent (Wen and He 2012; Zhang and Wang 2018), resulting in changes in the chemical properties of the pore water. However, it has been proven that the physicochemical effects of salt solutions have significant adverse effects on the SWRCs of fine-grained soils (Rao 1995; Thyagaraj and Rao 2010; Ravi and Rao 2013). Research results have shown that increasing the concentration of sodium chloride in solution decreases the water content at a certain suction level on the SWRCs of bentonite–sand mixtures (Ravi and Rao 2013). Similar results also were observed in the loam with different salt solutions (Xing et al. 2017). Changes in the chemical composition of the pore water produce noticeable effects on the stability of slopes that are covered by loess (Dijkstra et al. 1994; Wen and He 2012; Zhang et al. 2013, 2014), but very few studies have examined the effect of salt solutions on the hydraulic properties of loess in irrigated agricultural areas (Zhang and Zhang 2018). Little is known about the effects of various cations and the concentration of solutions on the SWRCs of loess in these environments.

The aim of this paper was to investigate the factors that affect the SWRCs of Chinese loess. Thus, we used a volumetric pressure plate extractor to determine the SWRCs of natural loess taken from six different spatial sites and soil layers that provided variations in mineral composition, initial water content, density, and grain size. We examined the remolded, artificially mixed, and salt-saturated loess to investigate the effects of the structure distribution, fine-grain fraction, coarse-grain fraction, and salt solution on the SWRCs of the samples. To better understand the factors that affect the SWRCs of loess, we performed various tests with samples of loess. These tests include determination of soil parameters, including index property, grain size distribution, specific surface area (SSA), and cation exchange capacity (CEC), XRD mineral composition, and scanning electron microscopy (SEM). Based on these results and analyses, a better understanding of the properties and behavior of the unsaturated loess was attained, and it was helpful in solving geotechnical problem and in mitigating the potential geohazard in the unsaturated loess.

Materials and methods

Materials

Samples

Six natural loess samples were taken from five sites where loess typically exists from west to east in the Chinese Loess Plateau. Five samples of Malan loess were taken, one each from Xining City in Qinghai Province, Xiji County in Ningxia Province, and three cities in Gansu Province, i.e., Lanzhou City, Tianshui City, and Longnan City. Another Lishi loess sample also was taken from Lanzhou City. In addition, to study the effect of coarse grains, sand was taken from the desert close to Minqing County in Gansu Province for the preparation of artificial loess samples. The sand sample was identified as S_{MQ}. The specific sites from which the loess samples were obtained are provided in Table 1 and in the KMZ supplementary file.

Based on the sites from which the samples were collected, the loess samples were identified as L_{XN}, L_{XJ}, L_{LZ1}, L_{LZ2}, L_{TS}, and L_{LN}, and their properties are summarized in Table 1. Their grain size distributions were determined using the dry sieve and sedimentation methods (JGS 2010). Figure 1 presents results of the tests. The semi-quantitative mineral compositions showed that quartz, calcite, and feldspar were the dominant minerals with smaller amounts of clay (Table 2). Loess samples typically are silty with a finer trend from the west to the east (Fig. 1).

Solutions

Previous studies have indicated that the ions from sodium chloride (i.e., Na^+ and Cl^- ions) are the predominant ions in the spring water in the Chinese agricultural irrigation areas and that K^+, Mg^{2+}, and Ca^{2+} also are common ions in the water (Wen and He 2012; Zhang et al. 2013; Zhang and Zhang 2018). Hence, two series of experiments were designed to study the effect of pore water chemistry on the SWRCs of salted loess. The aim of the first series of experiments was to examine the impact of the concentration of salt in the pore water with different concentrations of NaCl solutions (i.e., 3, 6, 10, 12, 14, and 16% by weight). The aim of the second series of experiments was to examine the effects of various types of cations in pore water. To do so, we dissolved potassium chloride (KCl), magnesium chloride ($MgCl_2$), and calcium chloride ($CaCl_2$) in de-aired, distilled water at concentrations of 1 mol/L.

Sample preparation

We performed four groups of experiments to study the factors that affected the soil–water retention curve of Chinese loess, including six undisturbed samples of loess, three remolded samples of loess, nine artificial samples of loess, and eleven samples of loess that had been treated with a salt solution.

Undisturbed loess samples

The six undisturbed loess samples were used to investigate the effect of the sampling site, which is essential for the different soil properties. The natural loess blocks were cut by a ring with an internal diameter of 6.18 cm and a height of 2 cm. The undisturbed loess samples were identified as L_{XNU}, L_{XJU}, L_{LZ1U}, L_{LZ2U}, L_{TSU}, and L_{LNU} according to their sampling sites, as mentioned in "Samples."

Table 1 Basic physicochemical properties of six natural loess

Property	L_{XN}	L_{XJ}	L_{LZ1}	L_{LZ2}	L_{TS}	L_{LN}
Specific gravity (Gs)	2.70	2.70	2.71	2.74	2.76	2.70
Initial moist density (g/cm^3)	1.43	1.55	1.47	1.44	1.62	1.43
Initial water content (%)	9.91	9.1	14.37	11.31	12.35	8.44
Liquid limit (%)	27.71	25.04	28.33	34.65	34.76	32.88
Plastic limit (%)	15.00	14.76	16.36	17.19	16.92	17.60
Plasticity index	12.71	10.28	11.97	17.58	17.58	15.27
Average grain size (mm)	0.015	0.021	0.021	0.011	0.018	0.025
SSA (m^2/g)	21.41	31.50	24.41	42.97	27.50	29.05
CEC (meq/100 g)	2.7	4.0	3.2	10.7	5.2	3.7

L_{XN}, Malan loess from Xining City in Qinghai Province (36.254°, 101.754°); L_{XJ}, Malan loess from Xiji County in Ningxia Province (35.954°, 105.703°); L_{LZ1}, Malan loess from Lanzhou City in Gansu Province (36.096°, 102.796°); L_{LZ2}, Lishi loess from Lanzhou City in Gansu Province (36.097°, 102.796°); L_{TS}, Malan loess from Tianshui City in Gansu Province (34.948°, 105.179°); L_{LN}, Malan loess of Longnan City in Gansu Province (34.663°, 104.713°)

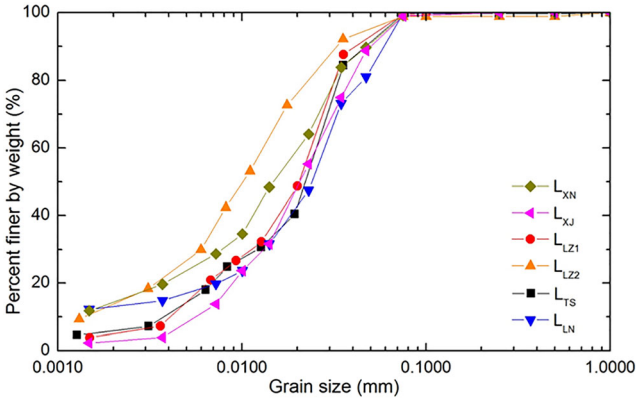

Fig. 1 Grain size distribution curves of the six natural samples

Remolded loess samples

The three identical samples of natural loess, i.e., L_{LZ1}, L_{TS}, and L_{LZ2}, were used to study the effect of disturbing the structure. First, the samples were air-dried and passed through a 1-mm sieve, after which they were oven-dried. This size of sieve was selected because the grain sizes of the samples were less than 1 mm. The oven-dried samples were wetted with water and sealed in a plastic bag for 24 h to achieve a uniform distribution of the moisture. Then, the wetted samples were placed in a specially designed cube mold with 7-cm sides. An automatic loading machine was used to prepare the square samples. To attain a uniform density, the samples were placed in three layers, and each layer was compacted to a designated dry density to achieve the same initial water content and dry density as the corresponding natural samples. Subsequently, the square samples were cut by the same cutting ring method. The three loess samples were termed as L_{LZ1R}, L_{TSR}, and L_{LZ2R}.

Artificial loess samples

Nine artificial loess samples were prepared to study the effects of the fine grain and the coarse grain on the SWRCs. For the fine-grain samples, the L_{TS} loess was mixed into the L_{LZ1} loess at different proportions. The mass percentages of the L_{TS} loess in the mixtures were 10%, 20%, 30%, 40%, and 50%, and the mixed samples were recorded as L_{T10}, L_{T20}, L_{T30}, L_{T40}, and L_{T50}, respectively. For the coarse-grain series, S_{MQ} sand was mixed with L_{LZ1} loess at different proportions. The mass percentages of sand were 5%, 10%, 20%, and 30%, and the corresponding mixtures were recorded as L_{S05}, L_{S10}, L_{S20}, and L_{S30}. The mixed samples were wet with water and sealed in a plastic bag for 24 h to achieve a uniform distribution of the moisture. Then, all of the samples of the artificial loess were obtained by the compaction technique and cutting, as described in "Undisturbed loess samples" and "Remolded loess samples." All of the artificial loess samples had almost the same initial dry density and water content. The index properties and grain size distributions were examined according to the methods suggested by the Japanese Geotechnical Society (JGS 2010). Their basic properties are listed in Table 3, and Fig. 2 is a plot of their grain size distribution curves. It is interesting to note that there was no continuous increase in the fine-grain fraction when the L_{TS} loess was mixed into the L_{LZ1} loess, while the artificial loess samples became coarser as the percentage content of sand increased. First, the results were related to the features of the grain. In addition, the non-continuous changes may have been related to the physicochemical effects that occurred in the process of mixing the L_{TS} and L_{LZ1} samples of loess, both of which had almost the same grain size distribution (Fig. 1).

Loess samples treated with a salt solution

The L_{LZ1} loess sample was used to study the effect of the salt solution on the SWRC, including the concentration of the salt and type of cations. The oven-dried and sieved L_{LZ1} loess samples were wetted using different salt solutions and sealed in a plastic bag for 24 h to achieve uniform distribution of the moisture. For the salt concentration series, the NaCl solutions used to treat the loess samples were identified as L_{NaCl00},

Table 2 Mineral compositions of six natural loess

Loess	Mass percent (%)									Clay portion (%)			
	Quartz	Calcite	Anorthose	K feldspar	Hornblende	Dolomite	Hematite	Gypsum	Clay content	I/S	I	K	C
L_{XN}	36.3	10.9	12.5	8.8	3.0	3.2	—	5.7	19.5	58	34	—	8
L_{XJ}	45.6	15.9	7.9	1.4	17.6	3.1	—	1.1	23.2	70	26	—	4
L_{LZ1}	47.8	12.7	8.8	2.5	—	5.6	1.0	—	21.5	56	35	4	5
L_{LZ2}	47.9	1.3	12.0	2.1	—	—	—	1.0	35.7	54	43	—	3
L_{TS}	40.6	12.7	6.7	—	4.4	6.8	0.9	4.1	23.8	46	45	9	—
L_{LN}	35.6	13.3	7.9	1.2	—	0.9	—	—	41.0	39	51	10	—

I/S, interlayered illite/smectite; *I*, illite; *K*, kaolinite; *C*, chlorite

Table 3 Basic physicochemical properties of mixed loess samples

Property	L_{T10}	L_{T20}	L_{T30}	L_{T40}	L_{T50}	L_{S05}	L_{S10}	L_{S20}	L_{S30}
Specific gravity	2.72	2.73	2.74	2.75	2.67	2.70	2.70	2.71	2.69
Liquid limit (%)	26.92	28.14	28.08	27.97	25.01	26.85	26.94	24.49	23.24
Plastic limit (%)	15.87	16.38	16.76	17.18	16.94	16.58	17.05	14.08	14.38
Plasticity index	11.05	11.76	11.33	10.79	8.08	10.28	9.89	10.41	8.87
Average grain size (mm)	0.015	0.0156	0.016	0.0162	0.017	0.264	0.294	0.324	0.415
SSA (m^2/g)	16.51	17.28	17.74	19.27	20.18	11.32	10.25	8.41	7.65
CEC (meq/100 g)	3.5	3.6	3.8	3.7	4.1	3.2	3.0	2.7	2.3

L_{T10}, L_{T20}, L_{T30}, L_{T40}, and L_{T50}: mixtures of L_{TS} Tianshui Malan loess and L_{LZ1} Lanzhou Malan loess in a weight percentage of 10%, 20%, 30%, 40%, and 50% of L_{TS}. L_{S05}, L_{S10}, L_{S20}, and L_{S30}: mixtures of S_{MQ} sand and L_{LZ1} Lanzhou Malan loess of Lanzhou in a weight percentage of 5%, 10%, 20%, and 30% of S_{MQ}

L_{NaCl03}, L_{NaCl06}, L_{NaCl10}, L_{NaCl12}, L_{NaCl14}, and L_{NaCl16}, which corresponded to the NaCl concentrations of 0%, 3%, 6%, 10%, 12%, 14%, and 16% by weight. For the cation type series, the loess samples treated with NaCl, KCl, $MgCl_2$, and $CaCl_2$ solutions were termed as L_{NaCl}, L_{KCl}, L_{MgCl2}, and L_{CaCl2}. The loess samples that were treated with the salt solution were compacted and cut in the same way as the artificial loess samples, thereby maintaining the almost same dry density and water content during preparation. Table 4 lists their basic properties. The grain size distributions of the treated loess samples still were examined using the dry sieve and sedimentation methods suggested by the Japanese Geotechnical Society (JGS 2010). Figure 3 shows the grain size distribution curves of all of the treated loess samples. The fine-grain fraction increased as the concentration of NaCl increased, which was due to the tighter arrangement that resulted from the decrease in the thickness of the double layer and the increase in attractive forces in the clay particles. This trend was consistent with the trends that were observed in similar tests of fine-grain soils (Picornell et al. 1990), and this finding also has been proved by previous studies performed with loess that had been treated in NaCl solutions (Zhang et al. 2013, 2014). The coarse-grain fraction increased with higher valency of the cations and the greater radii of the cations, causing the aggregate to have a larger size. In general, these changes can be attributed to the physicochemical effect between particles or aggregates due to the addition of the salt solution to the fine particle soils.

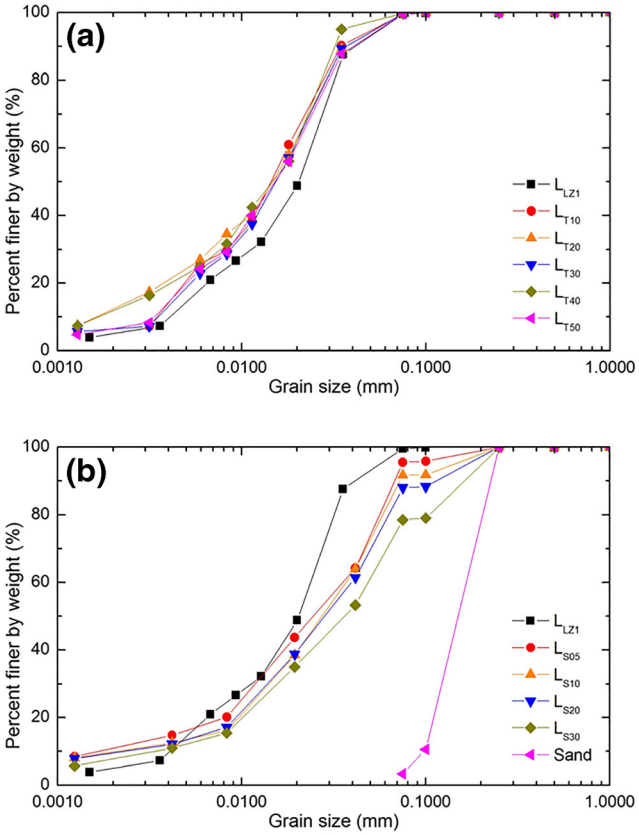

Fig. 2 Grain size distribution curves of the artificial loess samples. **a** Mixtures of L_{LZ1} loess and L_{TS} loess; **b** mixtures of L_{LZ1} loess and S_{MQ} sand

Test programs

Before the SWRC was measured using a pressure plate apparatus, all of the samples of loess were saturated in a humidor with a vacuum pumping system for 2 h. Then, distilled water and salt solutions were injected slowly into the sealed chamber until all of the samples were saturated. The saturation was calculated by measuring the masses of the samples before and after the saturation process. Table 5 provides the changes in the initial water content and the dry density for all of the samples. The loess samples with high concentrations of NaCl could not be thoroughly saturated. This was attributed to their lower hydraulic conductivity due to being tightly bound, which reduced the volume of the pores between the particles (Zhang and Zhang 2018).

The SWRCs of the loess samples were determined using a 15-bar pressure plate extractor. The saturated loess samples were placed in cutting rings described before on the high air-entry ceramic disk in the sealed air pressure chamber. Then, the samples were covered by a coarse porous stone and filter paper. The matric suction was controlled by increasing the air

Table 4 Basic physicochemical properties of salinized loess samples

Property	L_{NaCl00}	L_{NaCl03}	L_{NaCl06}	L_{NaCl10}	L_{NaCl12}	L_{NaCl14}	L_{NaCl16}	L_{NaCl}	L_{KCl}	L_{MgCl2}	L_{CaCl2}
Specific gravity (Gs)	2.71	2.72	2.73	2.74	2.74	2.74	2.74	2.74	2.72	2.53	2.67
Liquid limit (%)	28.33	27.60	26.72	25.49	24.68	24.53	24.08	25.49	27.00	25.66	21.08
Plastic limit (%)	16.36	15.94	15.98	15.20	14.30	13.92	13.80	15.20	15.94	15.23	13.11
Plasticity index	11.97	11.67	10.75	10.29	10.37	10.61	10.28	10.29	11.07	10.43	7.97
Average grain size (mm)	0.021	0.021	0.018	0.018	0.018	0.018	0.018	0.021	0.02	0.034	0.04
SSA (m^2/g)	24.41	29.05	28.29	25.10	24.16	23.55	22.94	25.10	18.04	18.66	21.71
CEC (meq/100 g)	3.2	3.7	3.6	3.2	3.1	3.0	2.9	3.2	2.9	2.5	3.9

L_{NaCl00}, L_{NaCl03}, L_{NaCl06}, L_{NaCl10}, L_{NaCl12}, L_{NaCl14}, and L_{NaCl16}: Lanzhou Malan loess treated with distill water and NaCl solution in a concentration of 3%, 6%, 10%, 12%, 14%, and 16%. L_{NaCl}, L_{KCl}, L_{MgCl2}, and L_{CaCl2}: Lanzhou Malan loess treated with NaCl, KCl, $MgCl_2$, and $CaCl_2$ solutions at 1 mol/L

pressure. The pore water was drained as the matric suction increased; equilibrium was reached when no additional water flowed out at the bottom of the ceramic disk. Normally, the elapsed time of the equilibrium state is approximately 3 days to 1 week, depending on the permeability of the samples. At the equilibrium condition, the loess samples were weighed, and the corresponding volumetric water contents were calculated to obtain the SWRCs.

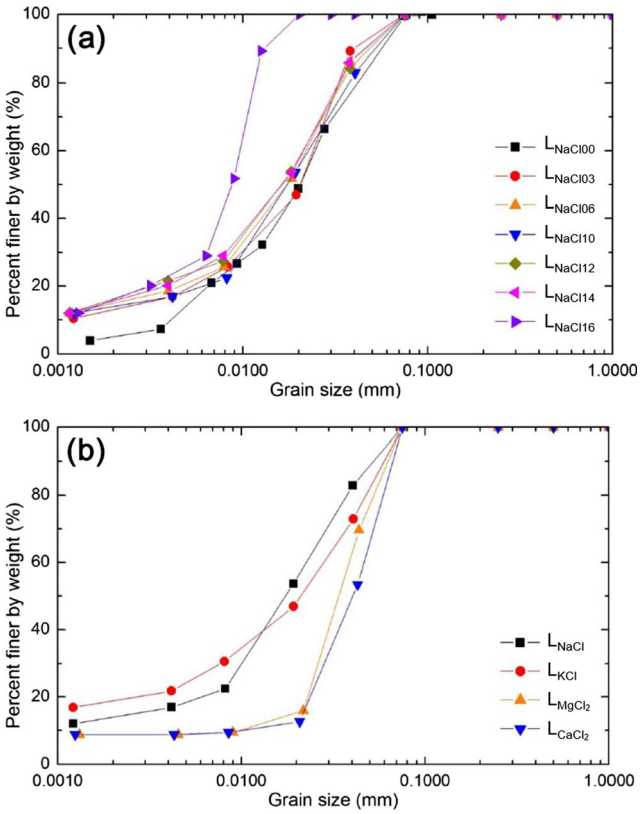

Fig. 3 Grain size distribution curves of the L_{LZ1} loess samples treated by salt solutions. **a** L_{LZ1} loess samples with different NaCl concentrations; **b** L_{LZ1} loess samples with different cations

Test results

SWRCs of the undisturbed loess

Figure 4 shows the SWRCs of the six natural loess samples from different sites and soil layers. The shapes of the SWRCs depend on the physical state and physical nature of the samples. For easy comparison, Fredlund (2000) distinguished different desaturation zones in SWRC, i.e., the boundary effect zone (0.1–0.6 kPa), the primary transition zone (0.6–10 kPa), the secondary transition zone (10–1050 kPa), and the residual state of unsaturation (> 1050 kPa). Figure 4 shows that the L_{LZ1U} loess sample had no visible zone from the boundary effect to the primary transition zone; however, the L_{LZ1U} Malan loess sample has a steep secondary transition zone. The L_{XNU}, L_{XJU}, and L_{LNU} Malan loess samples generally presented similar trends with increasing matric suction, and their SWRCs were relatively smooth. Also, there were little differences at the point close to the air-entry. The volumetric water content in the L_{XNU} loess sample decreased more rapidly than that in the L_{XJU} and L_{LNU} samples with increasing matric suction. This observation was related to the differences in their mineral content and structure and, consequently, the different physical states. Compared with the L_{XJU} and L_{LNU} samples, the L_{XNU} sample had the least clay content and the lowest initial density (Tables 1 and 2), resulting in a larger pore size and less cementation (Fig. 8). The results indicated that, even for the same layers of loess, slight changes in the physical state and physical nature can cause noticeable impacts on the shapes and trends of their SWRCs.

The SWRCs of the L_{LZ2U} Lishi and L_{TSU} Malan loess samples had no observed primary transition zone, and, in comparison with the SWRCs of the other four Malan samples, there was little change in the secondary transition zone. Figure 8 shows that their volumetric water contents deceased much slower with increasing matric suction than the volumetric water contents of the other four Malan samples, which was due to their denser packing and more cementation with

Table 5 Summary of pressure plate extractor test

Test no.	Test type	Before saturation			After saturation	
		ρ_i	w_i	e	V_W	S
Natural property effect (undisturbed)						
T_{01}	L_{XNU}	1.43	9.91	0.89	46.53	98.63
T_{02}	L_{XJU}	1.55	9.10	0.75	41.56	97.14
T_{03}	L_{LZ1U}	1.47	14.37	0.96	48.45	98.76
T_{04}	L_{LZ2U}	1.68	11.31	0.63	37.32	98.48
T_{05}	L_{TSU}	1.62	12.35	0.76	42.11	97.84
T_{06}	L_{LNU}	1.43	8.44	0.89	46.78	99.54
Structure disturbance effect (remolded)						
T_{07}	L_{ZL1R}	1.47	14.37	0.96	46.06	98.57
T_{08}	L_{TSR}	1.62	12.35	0.76	40.09	97.24
T_{09}	L_{LZ2R}	1.68	11.31	0.63	36.45	102.00
Fine-grain effect (artificial)						
T_{10}	L_{T10}	1.51	15.75	0.81	43.19	96.62
T_{11}	L_{T20}	1.50	15.36	0.83	43.42	96.00
T_{12}	L_{T30}	1.51	15.12	0.81	43.56	97.17
T_{13}	L_{T40}	1.51	15.77	0.82	43.34	96.23
T_{14}	L_{T50}	1.50	15.76	0.78	43.60	99.51
Coarse-grain effect (artificial)						
T_{15}	L_{S05}	1.49	15.66	0.81	41.73	93.25
T_{16}	L_{S10}	1.49	14.44	0.82	42.51	94.63
T_{17}	L_{S20}	1.51	14.39	0.80	41.53	93.75
T_{18}	L_{S30}	1.52	14.98	0.77	40.75	93.78
Salt concentration effect (remolded)						
T_{19}	L_{NaCl00}	1.52	17.85	0.81	44.41	99.47
T_{20}	L_{NaCl03}	1.51	17.52	0.80	41.83	93.89
T_{21}	L_{NaCl06}	1.52	17.67	0.80	41.23	92.84
T_{22}	L_{NaCl10}	1.52	17.46	0.80	40.82	91.63
T_{23}	L_{NaCl12}	1.52	17.98	0.80	40.45	91.35
T_{24}	L_{NaCl14}	1.52	17.92	0.80	39.98	89.40
T_{25}	L_{NaCl16}	1.52	17.15	0.80	39.44	89.24
Cation type effect (remolded)						
T_{26}	L_{NaCl}	1.51	13.60	0.74	40.24	94.47
T_{27}	L_{KCl}	1.52	14.55	0.79	43.33	98.06
T_{28}	L_{CaCl2}	1.52	14.29	0.75	41.62	96.91
T_{29}	L_{MgCl2}	1.52	13.62	0.67	39.27	98.02

ρ_i, initial dry density; w_i, initial water content; e, initial ratio void; V_W, volumetric water content; S, saturation

smaller pore space. The SWRCs of the L_{LZ2U} and L_{TSU} samples had no essential differences in the shapes or variation trends of their curves, and the curve of L_{LZ2U} was under the L_{TSU} curve. This was due mainly to the fact that the L_{TSU} sample had a higher initial density than the L_{LZ2U} sample (Table 1), as they had almost basic properties, i.e., Atterberg limits and structures (Table 1 and Fig. 8).

The five Malan loess samples that were collected at different sites had similar physical characteristics, such as grain size

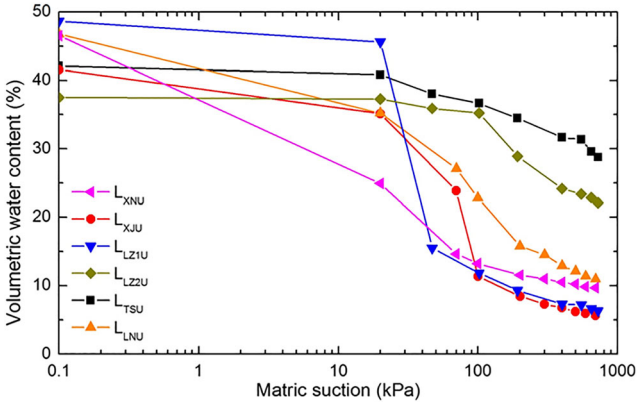

Fig. 4 Soil–water retention curves of undisturbed loess samples

distribution and mineral composition, but differences were observed in their physical states and structures. Hence, the changes in the SWRCs of the same loess layers can be attributed to their joint influences. For loess samples from different layers of soil, e.g., L_{LZ1U} and L_{LZ2U}, the physical characteristics, such as their mineral compositions, may be a key factor since the older strata have a greater clay content and fine grain, resulting in higher specific surface area and denser packing. These results suggest that the SWRCs of fine-grain soils depend on multiple factors. Hence, it is necessary to analyze the effect of the individual factors on SWRC.

SWRCs of remolded loess

Figure 5 compares the SWRCs of three undisturbed and remolded samples. Figure 5a shows the SWRCs of the undisturbed L_{LZ1U} and remolded L_{LZ1R} loess samples. The SWRC of L_{LZ1R} shows a steep decrease in volumetric water content at low matric suction, and no transition was observed for any of the desaturation zones. In addition, its shape was similar to the shapes of the L_{XNU}, L_{XJU}, and L_{LNU} Malan samples. The primary transition zone in the SWRC of L_{LZ1U} occurred above that of the SWRC of L_{LZ1R}. Subsequently, the SWRCs of L_{LZ1U} and L_{LZ1R} became almost the same in their secondary transition zone. However, the SWRC of L_{LZ1R} still showed a slightly higher volumetric water content than the SWRC of L_{LZ1U}. The SWRCs of the L_{TSU} and L_{TSR} loess samples (Fig. 5b) showed almost the same volumetric water content for the undisturbed and remolded loess samples in both the boundary effect zone and the primary transition zone, but, after that, the volumetric water content of the L_{TSR} sample decreased more rapidly than that of the L_{TSU} sample because the matric suction was increased at the secondary transition zone. Figure 5c shows that no differences were observed in SWRCs of the undisturbed and remolding L_{LZ2U} and L_{LZ2R} loess samples.

Because the same initial conditions were imposed, the undisturbed and remolded loess samples existed only in different structures, as shown in Fig. 9. For the L_{LZ} loess, the rapid

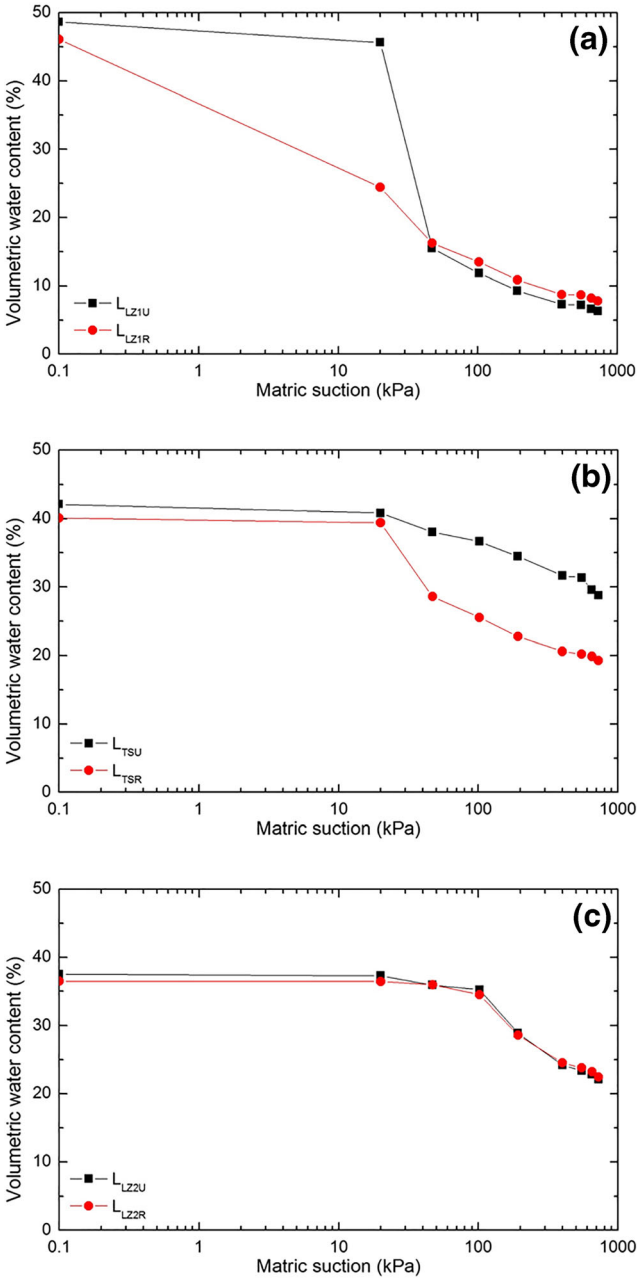

Fig. 5 Soil–water retention curves of undisturbed and remolded loess samples. **a** Undisturbed L_{LZ1U} and remolded L_{LZ1R} loess samples; **b** undisturbed L_{TSU} and remolded L_{TSR} loess samples; **c** undisturbed L_{LZ2U} and remolded L_{LZ2R} loess samples

decrease in volumetric water content at low matric suction is related to larger aggregates and, subsequently, larger inter-aggregate pores (i.e., pore space between aggregates) in the remolded L_{LZU} sample. However, in the secondary transition zone, the slight increase in the volumetric water content resulted from smaller intra-aggregate pores (i.e., pore space in an aggregate), as shown in Fig. 9a. As the matric suction increased, the more rapid decrease in the volumetric water content of the SWRCs of the L_{TSU} sample can be explained as follows. This was due to the very slightly greater size of inter- and intra-aggregate pores, resulting in the dispersion of the clay minerals (Fig. 9b). Although some structural changes were observed between the undisturbed and remolded L_{LZ2} loess samples, the remolding caused very little difference in the aggregate and its pores. As a result, no changes were observed in the SWRCs of either the L_{LZ2U} or the L_{LZ2R} loess samples. In general, the disturbance of the structure modified the size of the aggregate and its pores, and, as a result, the different SWRCs occurred in the undisturbed and remolded samples.

SWRCs of artificial loess at different grain size distributions

Figure 6 shows the effects of grain size on the SWRCs of the artificial loess samples. Figure 6a shows the effect of the fine grain on the SWRCs of the L_{LZ1} and L_{TS} samples. The shapes of the SWRCs were similar to the shape of the SWRC of the L_{LZ1R} sample, i.e., they were smooth curves that had a slowly descending trend. Moreover, the volumetric water contents of all the artificial loess samples were less than that of L_{LZ1R} at saturation. As a result, their volumetric water contents were higher than those of L_{LZ1R}. Figure 6b shows the effect of coarse grain on the SWRCs of the artificial samples produced by mixing L_{LZ1} loess and S_{MQ} sand. They had lower

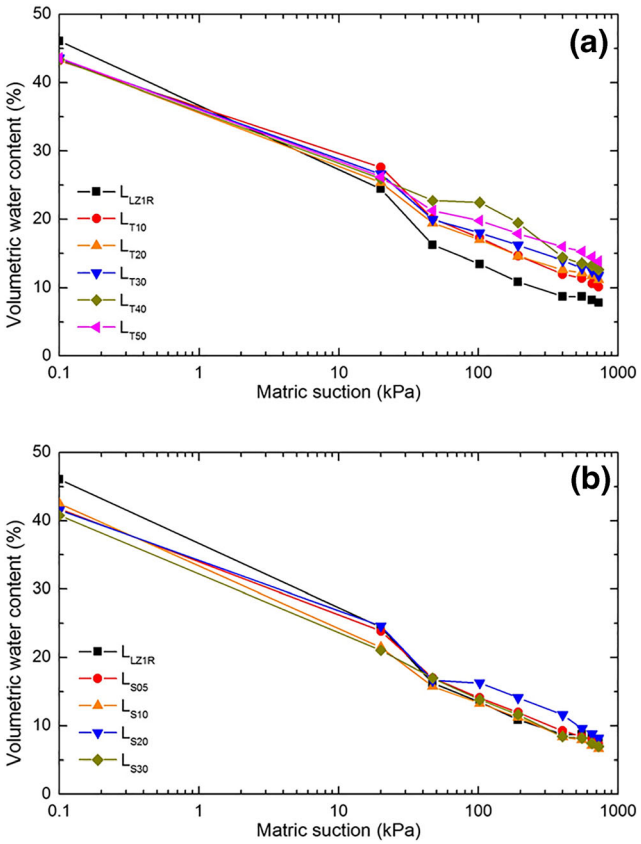

Fig. 6 Soil–water retention curves of artificial loess samples. **a** Mixtures of L_{LZ1} and L_{TS} loess; **b** mixtures of L_{LZ1} loess and S_{MQ} sand

volumetric water content at the low matric suction zone before 20 kPa. Subsequently, they only had a slight effect on the SWRCs of the artificial loess samples that had increasing fractions of coarse grain, which caused the increase in the volumetric water content at a given matric suction.

The volumetric water content of the SWRCs increased at each given matric suction when the L_{LZ1} loess was mixed with additional L_{TS} loess. As a result, the artificial loess samples had a higher specific surface area due to the increase in the fine-grain fraction (Table 3). As a result, the artificial loess with the finer grain sizes had the ability to hold more water during desaturation. In contrast, the artificial loess samples with coarser grain sizes had lower specific surface areas (Table 3), which resulted in weaker water retention capacity with increasing matric suction because the coarser grains and the smaller specific surface area resulted in larger pore space. It should be noted that the fine-grain fraction had a more prominent influence on the SWRCs of the artificial loess than the coarse-grain fraction.

SWRCs of remolded loess at different salt solutions

Figure 7a shows the effect of the concentrations of NaCl on the SWRCs of the remolded loess samples. They had shapes that were similar to the shapes of the remolded loess samples that were saturated by the NaCl solution at different concentrations, and they had a slower descent trend than the SWRCs of the remolded sample that was treated by distilled water (L_{NaCl00}). In addition, their foremost volumetric water contents generally were lower than that of the L_{NaCl00} sample. This was attributed to the fact that the loess samples had relatively low saturation with increasing salt concentration. After the boundary effect zone, the decrease in the volumetric water content of the remolded samples of loess saturated by NaCl solutions occurred more slowly than that of the L_{NaCl00} sample as the matric suction from the primary to the secondary transition zone was increased. As the concentrations of the NaCl increased, fewer changes occurred in the volumetric water contents of the samples at a given matric suction. This reflected the adjustment in the structure that was induced by changes in the ion concentration.

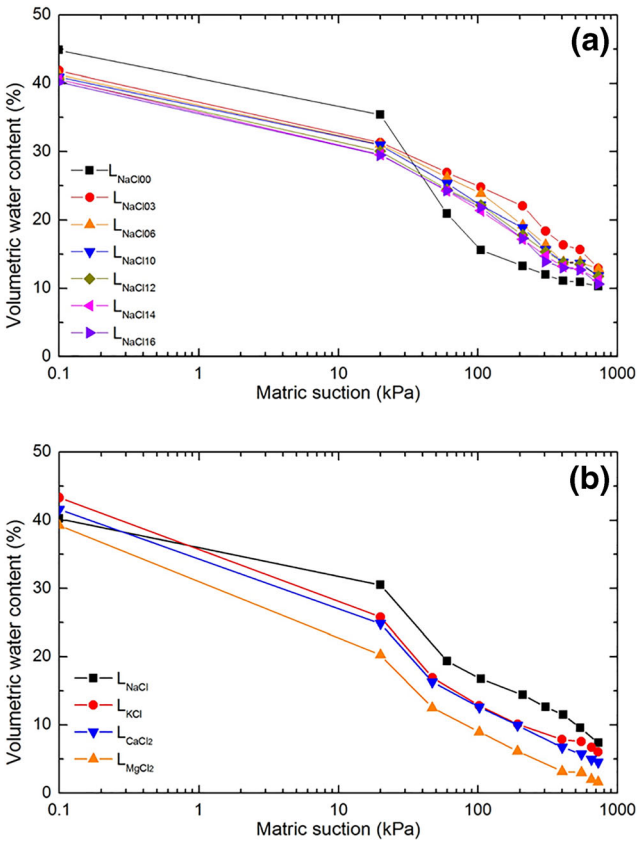

Fig. 7 Soil–water retention curves of remolded loess samples. **a** Samples saturated by different NaCl concentrations; **b** samples saturated by different cations

Figure 7b shows the effect of the types of cations on the SWRCs of the remolded loess samples. At a given matric suction, the volumetric water content became lower, following the increasing sequence of $Na^+ < K^+ < Ca^{2+} < Mg^{2+}$. This means that such changes are related to the valence and the radius of the hydrated ion, which impact the thickness of the double electrode layer of clay surface modifying soil structures. Generally, a smaller hydrated ionic radius and a higher valence can generate a more flocculated structure, resulting in smaller pore spaces in soils. Hence, the water retention capacity of the fine-grain soils is increased when the valence is higher and the hydrated ionic radius is smaller.

Discussion

Structural effects

As suggested by D'Elia and Picarelli (1998) and Feda (2004), structure is a combination of fabric, composition, and interparticle forces. Thus, structure is closely linked to the properties of a soil (Lambe and Whitman 1969; Mitchell and Soga 2006). Thus, it is very important to link the macroscopic behaviors and the microscopic characteristics, which are observed via a scanning electron microscope (SEM) as a general tool. Figure 8 shows the SEM images of six samples of undisturbed loess. The L_{XN}, L_{XJ}, and L_{LZ1} loess samples had similar microscopic structures (Fig. 8a–c), such as their shapes, their sizes, and the arrangement of particles or aggregates at the microscopic scale. In addition, the three samples have similar mineralogical and physical properties (Table 1 and Fig. 1). They have a bulk shape, and they have a chain structure, which mainly includes edge–face contacts with some micropores. Overall, the three samples have similar soil–water retention behaviors. However, the SWRC of the L_{LZ1} loess sample shows a steep decrease in the volumetric

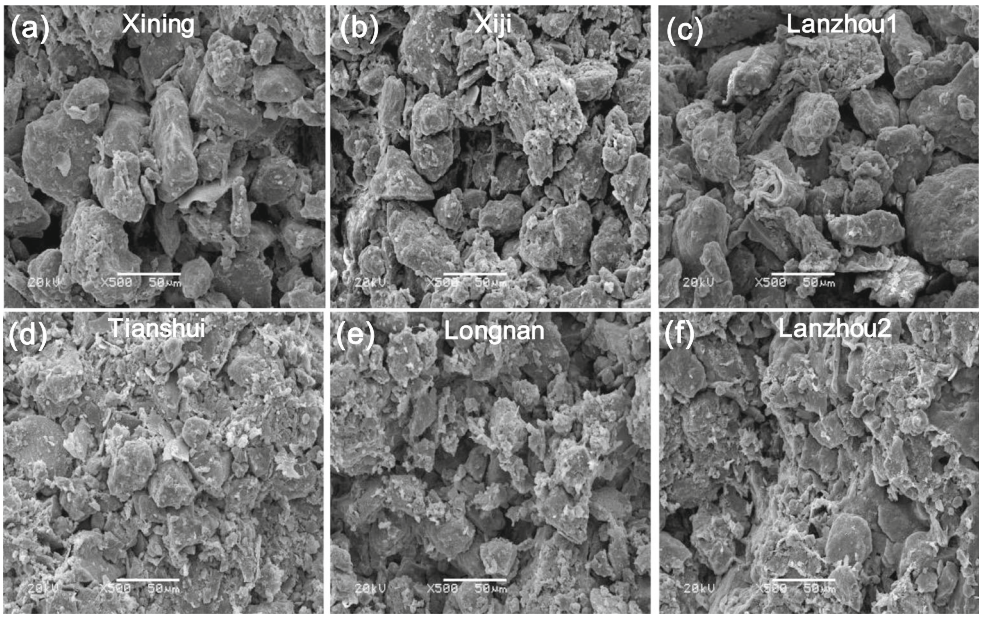

Fig. 8 SEM images of the six undisturbed samples. **a** L_{XJ} Xiji Malan loess; **b** L_{XN} Xining Malan loess; **c** L_{LZ1} Lanzhou Malan loess; **d** L_{TS} Tianshui Malan loess; **e** L_{LN} Longnan Malan loess; **f** L_{LZ2} Lanzhou Lishi loess

water content in the transition zone. This may be related to its small amounts of clay minerals and clay particles, resulting in a relatively loose packing with more micropore space. The SWRC of the L_{LN} loess sample was similar to those of the L_{XN}, L_{XJ}, and L_{LZ1} loess samples. However, it had a slighter decrease in the secondary transition zone because the L_{LN} loess sample contained more clay, which caused more cementation between particles and aggregates (Figs. 1 and 8e). The L_{TS} Malan and L_{LZ2} Lishi loess samples were taken from different loess layers, but they had similar structures (Fig. 8d and f). The two loess samples had dense packing with small pore spaces, along with much clay cementation. Thus, their volumetric water content decreased very slowly with increasing matric suction in the secondary transition zone. The L_{LZ2} Lishi loess sample that was deposited in an older soil layer was compared with the L_{TS} Malan loess sample, and it was found to have more clay and fine-grain contents. However, the SWRC of the L_{LZ2} loess was close to those of the other four Malan loess samples. And here have the most significant differences to the secondary transition zone of L_{TS} loess sample, which is a low initial density (Table 1). These results suggest that the microstructure of the soil depends on its mineral composition, grain size, and in situ physical state.

Figure 9 shows the differences between the SEM images of the undisturbed samples and the remolded samples. The structure disturbance in the L_{LZ1} Malan remolded loess sample

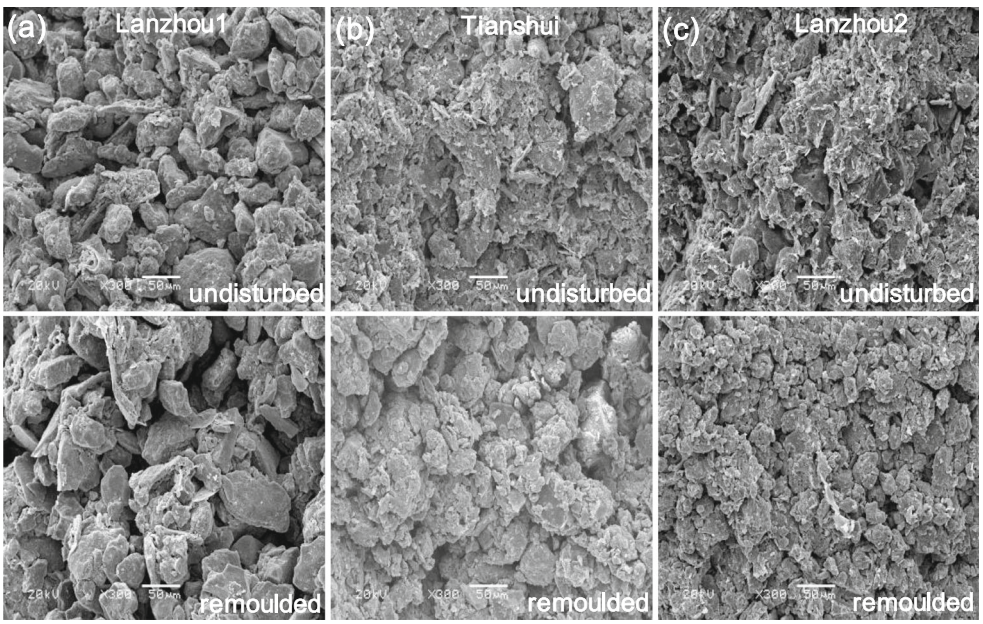

Fig. 9 SEM images of the three undisturbed and remolded samples. **a** L_{LZ1} Lanzhou Malan loess; **b** L_{TS} Tianshui Malan loess; **c** L_{LZ2} Lanzhou Lishi loess

resulted in larger aggregates and, correspondingly, larger inter-aggregate pore spaces (Fig. 9a). As a result, the decrease in the volumetric water content at low matric suction is easier in the remolded L_{LZ1R} loess than in the undisturbed L_{LZ1U} loess.

Figure 9b and c compare the differences between the microstructures of the L_{TS} Malan and the L_{LZ2} Lishi loess samples before and after disturbances. A disturbance breaks the clay cementation between particles and aggregates, thereby changing the microstructures of the samples. The remolded L_{TSR} loess sample had more intra-aggregate pores than the undisturbed L_{TSU} loess. This explains why the decrease in the volume of water content in the L_{TSR} loess sample was more rapid than that in the L_{TSU} loess sample. Even the clay cementation in the undisturbed L_{LZ2} loess sample was destroyed, but the remolded L_{LZ2} loess sample still maintained its dense packing due to its high content of clay. Hence, the SWRCs of the undisturbed and remolded loess samples have no apparent change. The results indicated that pore size has a different effect on the different stages of desaturation of the SWRCs. The inter-aggregate pore behaves as a stronger influence in the boundary effect zone, and the intra-aggregate has a greater impact in the transition zone.

Physicochemical effects

The specific surface area (SSA) and cation exchange capacity (CEC) of soils are very important for understanding the surface properties of particles, and they also are crucial parameters in the prediction of the behaviors of soils. When the L_{TS} loess sample was added to the L_{LZ1} sample, the result was higher SSA and CEC values (Table 3). Thus, such a mixture can retain more water in the pores of the soil. However, additional energy is required to remove the water during desaturation. Hence, at a given matric suction, the volumetric water content is lower in the SWRCs of the mixtures of L_{LZ1} and L_{TS} loess, and it decreases as the fine-grain fraction increases to a critical value. Subsequently, the L_{TS} loess sample dominates the change in volumetric water content due to its increased matric suction. This finding is similar to that observed by Gao and Sun (2017).

For mixtures of L_{LZ1} loess and S_{MQ} sand, even though their SSA and CEC regularly become smaller as the S_{MQ} coarse-grain fraction increases, their behavior with respect to soil–water retention has no apparent changes. This is because there are no marked differences in the structures of the mixed loess samples while the coarse grain is being added. Hence, the SWRCs of the samples with different S_{MQ} sand fractions (i.e., L_{LZ1R}, L_{S05}, L_{S10}, L_{S20}, and L_{S30}) are almost the same.

Pore water chemistry effects

The pore water chemistry influences the hydro-mechanical behaviors of soils through the changes in the structures of the soil (Hawkins and Anson 1998; Montoro and Francisca 2010) that are caused by the compression of the diffused double layer and the re-arrangement of particles (Moore 1991; Wang and Siu 2006). The thickness of the diffused double layer has a negative correlation with the concentration of cations and the valence of the pore water, and it is related positively to the ionic radius (Moore 1991; Rao 1995). Consequently, the compression of the diffused double layer reduces the diameters of the pores by reducing the distance between particles (Nagaraj and Murthy 1983). Hence, the volumetric water content of a loess sample that is saturated with distilled water (L_{NaCl00}) is higher than that of loess samples saturated by various concentrations of NaCl solutions (L_{NaCl03}, L_{NaCl06}, L_{NaCl10}, L_{NaCl12}, L_{NaCl16}) in the boundary effect zone of SWRCs. The compression of the diffusion layer and the decrease of adsorbed water also are significant as the valence of the cations increases. Thus, the volumetric water content of the L_{CaCl2} and L_{MgCl2} loess samples at a critical matric suction was lower than that of the L_{NaCl} and L_{KCl} samples.

Previous studies have shown that the addition of the NaCl solution changes the arrangement of the particles in the structure of the soil from face to face to edge to face due to the increase in the electrostatic repulsion between the particles (Zhang et al. 2014). This explains the decrease in the slopes of the primary transition zone in SWRCs after the addition of the NaCl solution. The pore water chemistry can modify the structure of fine-grain soils, including the forces and arrangements between particles or aggregates.

Conclusions

To study the factors that affect the SWRCs of Chinese loess, we performed a series of pressure plate extractor tests on the undisturbed, artificial, and remolded loess samples saturated by distilled water and salt solutions. Based on the test results presented above, we reached the following conclusions:

1. The five Malan undisturbed loess samples have almost the same physical natures and different physical states and structures, resulting in the change in their SWRCs. However, their physical characteristics, such as mineral composition and grain features, have a significant impact on the SWRCs of the Lishi and Malan undisturbed loess samples from different layers of soil.
2. The effect of the disturbance of the structures on the SWRCs of the remolded loess samples depends on the types of loess, because they produce different aggregate sizes and different inter- and intra-aggregate pores during remolding. The modification is related mainly to the diffusion of the clay mineral and original damage to the cementation.

3. The effect of grain size on the SWRCs of the artificial loess samples is related to the fine-grain and coarse-grain fractions, which cause the changes in the features of the grain and the size of the pores. When the artificial loess samples have a greater fine-grain fraction, they can acquire more water at a given suction due to their higher specific surface area and smaller pore space. The fine-grain fraction has a more prominent influence on the SWRCs of the artificial loess than the coarse-grain fraction.
4. The effect of the salt solution on the SWRCs of the remolded loess is related to adjustment of the structure due to different concentrations, valences, and radii of the hydrated ions because the addition of the salt solution modifies the interparticle forces of the soils and, consequently, the changes in arrangement and pore between particles or aggregates.

Acknowledgments Yao Jiang acknowledges support from the CAS Pioneer Hundred Talents Program.

Funding information This study was supported by the National Key Research and Development Program of China (No. 2018YFC1504702), the National Natural Science Foundation of China (Nos. 41977212 and 41927806), and the Fundamental Research Funds for the Central Universities (No. lzujbky-2020-kb46).

References

Aldaood A, Bouasker M, Al-Mukhtar M (2015) Soil–water characteristic curve of gypseous soil. Geotech Geol Eng 33:123–135

Aubertin M, Mbonimpa M, Bussière B, Chapuis RP (2003) A model to predict the water retention curve from basic geotechnical properties. Can Geotech J 40:1104–1122

Brooks RH, Corey AT (1966) Properties of porous media affecting fluid flow. J Irrig Drain Div Am Soc Civ Eng 92:61–88

Cubrinovski M, Ishihara K (2002) Maximum and minimum void ratio characteristics of sands. J Jpn Geotechn Soc: Soils Found 42:65–78

D'Elia B, Picarelli L, Leroueil S, Vauna J (1998) Geotechnical characterisation of slope movements in structurally complex clay soils and stiff jointed clays. Italian Geotech J 32:5–32

Derbyshire E (2001) Geological hazards in loess terrain, with particular reference to the loess regions of China. Earth Sci Rev 54:231–260

Dijkstra T, Rogers CDF, Smalley IJ, Derbyshire E, Li YJ, Meng XM (1994) The loess of north-central China: geotechnical properties and their relation to slope stability. Eng Geol 36:153–171

Dijkstra T, Wasowski J, Winter M, Meng X (2014) Introduction to geohazards of Central China. Q J Eng Geol Hydrogeol 47:195–199

Feda J (2004) Physical models of soil behaviour. Eng Geol 72:121–129

Fredlund D (2000) The 1999 R.M. Hardy Lecture: the implementation of unsaturated soil mechanics into geotechnical engineering. Can Geotech J 37:963–986

Fredlund D, Rahardjo H (1993) Soil mechanics for unsaturated soils. Wiley

Fredlund DG, Xing Q (1994) Equations for the soil-water characteristic curve. Can Geotech J 31:521–532

Gallipoli D, Wheeler SJ, Karstunen M (2003) Modelling the variation of degree of saturation in a deformable unsaturated soil. Géotechnique 53:105–112

Gao Y, Sun D (2017) Soil-water retention behavior of compacted soil with different densities over a wide suction range and its prediction. Comput Geotech 91:17–26

Hawkins, A., Anson, R., 1998. The effect of calcium ions in pore water on the residual shear strength of kaolinite and sodium montmorillonite. Geotechnique 52, págs. 379–381

Huang M, Fredlund D, Fredlund M (2010) Comparison of measured and PTF predictions of SWCCS for loess soils in China. Geotech Geol Eng 28:105–117

James M, Benson C, Lisa R (1997) Soil-water characteristic curves for compacted clays. J Geotech Geoenviron 123:1060–1069

JGS (2010) Basic handbook of the soil testing, 2th Edition, Japanese Geotechnical Society, (in Japanese)

Jiang M, Hu H, Liu F (2012) Summary of collapsible behaviour of artificially structured loess in oedometer and triaxial wetting tests. Can Geotech J 49:1147–1157

Jiang Y, Chen W, Wang G, Sun G, Zhang F (2017) Influence of initial dry density and water content on the soil–water characteristic curve and suction stress of a reconstituted loess soil. Bull Eng Geol Environ 76:1085–1095

Juang CH, Dijkstra T, Wasowski J, Meng X (2019) Loess geohazards research in China: advances and challenges for mega engineering projects. Eng Geol 251:1–10

Lambe T, Whitman R (1969) Soil mechanics. John Wiley & Sons, Inc

Leong EC, Rahardjo H (1997) Review of soil-water characteristic curve equations. J Geotech Geoenviron 123:1106–1117

Li P, Li T, Vanapalli SK (2016) Influence of environmental factors on the wetting front depth: a case study in the Loess Plateau. Eng Geol 214: 1–10

Li P, Li T, Vanapalli SK (2018) Prediction of soil–water characteristic curve for Malan loess in Loess Plateau of China. J Cent South Univ 25:432–447

Lin Z, Liang W (1982) Engineering properties and zoning of loess and loess-like soil in China. Can Geotech J 19:76–91

Liu T (1985) Loess and the environment. Science Press, Beijing

Liu Z, Liu F, Ma F, Wang M, Bai X, Zheng Y, Yin H, Zhang G (2016) Collapsibility, composition, and microstructure of loess in China. Can Geotech J 53:673–686

Lourenço S, Saulick Y, Zheng S, Kang H, Liu D, Lin H, Yao T (2017) Soil wettability in ground engineering: fundamentals, methods, and applications. Acta Geotech:1–14

Lu N, Likos WJ (2004) Unsaturated soil mechanics

Mitchell JK, Soga K (2006) Fundamentals of soil behavior, 3rd Edition. John Wiley & Sons, Inc

Montoro M, Francisca F (2010) Soil permeability controlled by particle–fluid interaction. Geotech Geol Eng 28:851–864

Moore R (1991) The chemical and mineralogical controls upon the residual strength of pure and natural clays. Geotechnique 41:35–47

Mu Q, Dong H, Liao H, Dang Y, Zhou C (2020) Water-retention curves of loess under wetting–drying cycles. Géotechn Lett 10:1–6

Muñoz-Castelblanco J, Pereira J, Delage P, Cui Y (2012) The water retention properties of a natural unsaturated loess from northern France. Géotechnique 62:95–106

Nagaraj T, Murthy B (1983) Rationalization of Skempton's compressibility equation. Géotechnique 33:433–443

Ng C, Sadeghi H, Hossen S, Chiu C, Alonso E, Baghbanrezvan S (2016) Water retention and volumetric characteristics of intact and re-compacted loess. Can Geotech J 53:1258–1269

Oades J, Waters A (1991) Aggregate hierarchy in soils. Aust J Soil Res 29:815–828

Pedarla A, Acharya R, Bheemasetti T, Puppala A, Hoyos L (2015) Influence of mineral montmorillonite on soil suction modeling parameters of natural expansive clays. Indian Geotechn J:1–8

Picornell M, El-furf Q, Rahim M (1990) Effects of small concentrations of soluble salts on hydrometer analysis. In: Lamb, K.B.H.a.R.O. (Ed.), Physico-chemical aspect of soil and related material. ASTM STP 10095, American Society for Testing and Material, pp. 185–195

Puppala A, Punthutaecha K, Vanapalli S (2006) Soil-water characteristic curves of stabilized expansive soils. J Geotech Geoenviron 132: 736–751

Rahardjo H, Satyanaga A, D'Amore G, Leong E (2012) Soil–water characteristic curves of gap-graded soils. Eng Geol 125:102–107

Rao SN (1995) Effects of exchangeable cations on hydraulic conductivity of a marine clay. Clay Clay Miner 43:433–437

Ravi K, Rao S (2013) Influence of infiltration of sodium chloride solutions on SWCC of compacted bentonite–sand specimens. Geotech Geol Eng 31:1291–1303

Tarantino A (2009) A water retention model for deformable soils. Géotechnique 59:751–762

Thyagaraj T, Rao S (2010) Influence of osmotic suction on the soil-water characteristic curves of compacted expansive clay. J Geotech Geoenviron 136:1695–1702

van Genuchten M (1980) A closed-form equation of predicting the hydraulic conductivity of unsaturated soils. Soil Sci Soc Am J 44:892–898

Wang Y, Siu W (2006) Structure characteristics and mechanical properties of kaolinite soils. II. Effects of structure on mechanical properties. Can Geotech J 43:601–617

Wen B, He L (2012) Influence of lixiviation by irrigation water on residual shear strength of weathered red mudstone in Northwest China: implication for its role in landslides' reactivation. Eng Geol 151:56–63

Xing X, Kang D, Ma X (2017) Differences in loam water retention and shrinkage behavior: effects of various types and concentrations of salt ions. Soil Tillage Res 167:61–72

Yilmaz Y, Mollamahmutoglu M (2009) Characterization of liquefaction susceptibility of sands by means of extreme void ratios and/or void ratio range. J Geotech Geoenviron 135:1986–1990

Zapata C, Houston W, Houston S, Walsh KD (2000) Soil–water characteristic curve variability. Geo-Denver:84–124

Zhang F, Wang G (2018) Effect of irrigation-induced densification on the post-failure behavior of loess flowslides occurring on the Heifangtai area, Gansu, China. Eng Geol 236:111–118

Zhang F, Zhang J (2018) Effects of pore water chemistry on hydraulic conductivity of saturated loess. Lowland Technol Int 20:27–36

Zhang S, Lövdahl L, Grip H, Tong Y (2007) Soil hydraulic properties of two loess soils in China measured by various field-scale and laboratory methods. CATENA 69:264–273

Zhang F, Wang G, Kamai T, Chen W, Zhang D, Yang J (2013) Undrained shear behavior of saturated loess with different concentrations of sodium chlorate solution. Eng Geol 155:69–79

Zhang F, Wang G, Kamai T, Chen W (2014) Effect of pore water chemistry on undrained shear behaviour of saturated loess. Q J Eng Geol Hydrogeol 47:201–210

Zhang F, Pei X, Yan X (2018) Physicochemical and mechanical properties of lime-treated loess. Geotech Geol Eng 36:685–696

Zhang F, Yan B, Feng X, Lan H, Kang C, Lin X, Zhu X, Ma W (2019) A rapid loess mudflow triggered by the check dam failure in a bulldoze mountain area, Lanzhou, China. Landslides 16:1981–1992

Zlatovic S, Ishihara K (2008) Normalized behavior of very loose nonplastic soils: effects of fabric. Soils Found 37:47–56